



Crista Galli Morphometry and Morphology in Sagittal Skeletal Malocclusions: A Retrospective Cross-Sectional Study

Taner Ozturk^{1-a*}, Yunus Emre Ucaker^{1-b}, Aykagan Cukurluoglu^{2-c}

¹ Department of Orthodontics, Faculty of Dentistry, Erciyes University, Kayseri, Türkiye.

² Department of Oral and Maxillofacial Radiology, Faculty of Dentistry, Erciyes University, Kayseri, Türkiye.

*Corresponding author

Research Article

History

Received: 09/04/2024

Accepted: 16/10/2024

ABSTRACT

Objective: This study aimed that examine the relationship between crista galli (CG) morphometry and morphology in different types of sagittal skeletal malocclusion.

Material-Methods: A total of 45 individuals included in the study were examined by dividing them into three subgroups Class I, Class II, and Class III, which included an equal number of samples according to the ANB°. In this study, different morphologies (teardrop, tubular, ossified) and morphometric (length, width, height) measurements of the CG were analyzed in adult patients with different sagittal malocclusions.

Results: When linear measurements of the CG were evaluated, no difference was found between skeletal malocclusion classes in terms of width and height. Crista galli length is significantly larger in Class I individuals (13.13±1.93 mm) than in Class III individuals (11.56±1.26 mm). On the other hand, the CG length of Class I and Class II individuals (11.67±2.28 mm) is similar. There is no significant relationship between crista galli morphology, Keros classification and CG pneumatization and skeletal malocclusion groups.

Conclusion: The anteroposterior CG length of skeletal class III individuals is less than that of skeletal class I individuals. Crista galli morphology does not differ according to sagittal skeletal malocclusions.

Keywords: Cone-Beam Computed Tomography, Malocclusion, Skull Base.

Sagittal İskeletsel Maloklüzyonlarda Crista Galli Morfometri ve Morfolojisi: Bir Retrospektif Kesitsel Çalışma

Research Article

Süreç

Geliş: 09/04/2024

Kabul: 16/10/2024

ÖZ

Amaç: Bu çalışmada farklı sagittal iskelet maloklüzyonu tiplerinde crista galli (CG) morfometrisi ve morfolojisi arasındaki ilişkinin incelenmesi amaçlandı.

Gereç-Yöntem: Çalışmaya dahil edilen toplam 45 birey, ANB°'ye göre eşit sayıda örnek içeren Sınıf I, Sınıf II ve Sınıf III olmak üzere üç alt gruba ayrılarak incelendi. Bu çalışmada, farklı sagittal iskeletsel maloklüzyona sahip erişkin hastalarda crista galli'nin farklı morfolojileri (gözyaşı, tübüler, kemikleşmiş) ve morfometrik (uzunluk, genişlik, yükseklik) ölçümleri analiz edildi.

Bulgular: Crista galli'nin lineer ölçümleri değerlendirildiğinde, iskeletsel maloklüzyon sınıfları arasında genişlik ve yükseklik açısından fark bulunamadı. Crista galli uzunluğu Sınıf I bireylerde (13,13±1,93 mm), Sınıf III bireylerde (11,56±1,26 mm) göre önemli ölçüde daha büyüktür. Buna karşın Sınıf I ile Sınıf II bireylerin (11,67±2,28 mm) CG uzunluğu benzer büyüklüktedir. Crista galli morfolojisi, Keros sınıflandırması ve crista galli pnömatizasyonu ile iskeletsel maloklüzyon grupları arasında anlamlı bir ilişki bulunmadı.

Sonuç: İskeletsel III bireylerin ön-arka crista galli uzunluğu iskeletsel sınıf I bireyler göre daha azdır. Crista galli morfolojisi sagittal iskeletsel maloklüzyona göre farklılık göstermez.

Anahtar Kelimeler: Konik Işınli Bilgisayarlı Tomografi, Kafa Tabanı, Maloklüzyon.

License



This work is licensed under
Creative Commons Attribution 4.0
International License

^a tanertr35@gmail.com

^c aykagann@gmail.com

^b <https://orcid.org/0000-0003-1670-286X>

^b dtyunusemreucaker@hotmail.com

^b <https://orcid.org/0009-0006-8683-9588>

How to Cite: Ozturk T, Ucaker YE, Cukurluoglu A. (2024) Crista Galli Morphometry and Morphology in Sagittal Skeletal Malocclusions: A Retrospective Cross-Sectional Study, Cumhuriyet Dental Journal, 27(4):222-229.

Introduction

The crista galli (CG) is a smooth, thick, pyramidal bone protrusion that extends sagittally in the shape of a rooster's crest in the front and middle of the lamina cribrosa of the ethmoid bone, one of the bones in the neurocranium.¹ The falx cerebri is attached to this anatomical formation, which is an important landmark in the anterior cranial fossa.² The location and features of the CG mean it has an important place in anterior skull base (e.g., hypophysis gland) surgical procedures and endoscopic sinus (e.g., ethmoid, frontal sinus) surgery.³⁻⁵ It can also show pneumatization because it is in the pneumatized ethmoid bone structure. It has been examined in studies on sex determination.⁶⁻⁸ Sagittal skeletal malocclusions have an important place in orthodontic practice. They provide classification by indicating the positions of the maxilla and mandible relative to the skull base and each other.⁹ Cranial anatomical structures, which were previously evaluated with two-dimensional images, are now more frequently examined with three-dimensional methods.^{2,9-11} In addition, with the development of multidisciplinary relationships, opportunities to examine normal anatomy or problems from a broad perspective rather than examining a small focal point have also improved.¹¹⁻¹³ One of the three-dimensional imaging methods used to examine the anatomy, structure, pathology, and variations of the craniofacial region is cone-beam computed tomography (CBCT).¹² It offers the advantages of lower radiation exposure, reduced artifacts, cost-effectiveness, and ease of use compared to computed tomography (CT) imaging, which is known as the gold standard and is more accessible.¹⁴ The relationship between sagittal skeletal anomalies and craniofacial region structures and anomalies has long been studied.^{9,12,15} The relationship between skeletal malocclusions and paranasal sinuses has also been examined previously.^{12,16} However, the relationship between malocclusions and the CG, a structure very close to the paranasal sinuses, has not yet been examined. Therefore, this study aimed to examine the relationship between CG morphometry and morphology in various types of sagittal skeletal malocclusion by examining

CBCT images. The null hypothesis was that CG morphometry and morphology would not differ across different sagittal skeletal malocclusion types.

Materials and Methods

This was a retrospective cross-sectional study. Before starting the study, permission for the protocol was obtained from the Clinical Research Ethics Committee of Erciyes University, dated 10th May 2023 with decision number 2023/338. All examinations were performed following the Declaration of Helsinki protocol, and informed consent forms were obtained from all patients before the study. This study examined the morphometry and classified the morphology of the CG in adult patients with various sagittal malocclusions. A power analysis (for 95% power, $d = 1.67$ and $\alpha = 0.05$ margin of error) performed with G*Power software (ver. 3.0.10, Franz Faul, Universität Kiel, Germany) determined that 11 patients were required in each group.⁷ The inclusion criteria were patients with CG formation on CBCT recordings; patients without craniofacial deformity, trauma, syndrome, orthodontic treatment, or surgical history; high-quality image content; and patients in whom the nasion, maxillary, and mandibular regions were clearly observed to determine the sagittal skeletal malocclusion.

Classification of Orthodontic Malocclusion

For individuals with cephalometric radiography, cephalometric evaluation was performed. For individuals without cephalometric radiography, cephalometric evaluation was carried out from the middle point of the sagittal plane sections of images taken with CBCT, which included the mandible (Point B) and maxilla (Point A) and the nasion structure (nasion point). The classification of malocclusion in the sagittal dimension was performed using the ANB°.¹⁷ A total of 45 individuals were divided into three subgroups: Class I (mean ANB: $1.83 \pm 1.29^\circ$; 7 males, 8 females), Class II (mean ANB: $7.35 \pm 2.07^\circ$; 5 males, 10 females), and Class III (mean ANB: $-4.13 \pm 2.03^\circ$; 5 males, 10 females), which included equal numbers of samples according to the ANB° (Table 1).

Table 1. Comparisons of crista galli morphometry and morphology of different skeletal malocclusion classes.

		Skeletal Class I (n=15)	Skeletal Class II (n=15)	Skeletal Class III (n=15)	P values	
	Age	18.7±8.6 ^a	24.7±8.0 ^b	22.7±7.6 ^{a,b}	0.020 * KW	
	ANB	1.83±1.29 ^a	7.35±2.07 ^b	-4.13±2.03 ^c	<0.001 *** OWA	
	SN/GoGn	33.89±5.35 ^a	44.49±9.18 ^b	35.24±9.64 ^a	0.003 ** OWA	
Gender	Male	7 (46.7)	5 (33.3)	3 (20.0)	0.031 * P	
	Female	8 (53.3)	10 (66.7)	12 (80.0)		
CG Linear Measurements	Length	13.13±1.93 ^a	11.67±2.28 ^{a,b}	11.56±1.26 ^b	0.048 * KW	
	Width	4.68±1.52	4.71±1.45	5.05±1.65		0.782 ^{OWA}
	Height	14.25±2.21	13.53±2.68	13.39±2.86		0.595 ^{OWA}
CG Morphology	Tear Drop	5 (33.3)	10 (66.7)	10 (66.7)	0.343 ^P	
	Tubular	8 (53.3)	4 (26.7)	4 (26.7)		
Keros Classification	Ossified	2 (13.3)	1 (6.7)	1 (6.7)	0.925 ^P	
	Type I	3 (20.0)	2 (13.3)	3 (20.0)		
	Type II	10 (66.7)	12 (80.0)	10 (66.7)		
Pneumatization	Type III	2 (13.3)	1 (6.7)	2 (13.3)	0.594 ^P	
	Present	0 (0.0)	1 (6.7)	1 (6.7)		
	Absent	15 (100.0)	14 (93.3)	14 (93.3)		

Numeric data was given Mean ± Standard Deviation. Categorical data was given Count (Percentage). P: Pearson Chi-Square test. KW: Kruskal-Wallis H test. OWA: One-Way ANOVA test. Statistically significant degree was given $p < 0.05$. *P < 0.05; **P < 0.01; ***P < 0.001.

Cephalometric Analysis Parameters

In performing cephalometric analyses, hard tissue points nasion (N), anterior nasal spine (ANS), sella (S), gonion (G), condylion (Co), gnathion (Gn), A point (A) and B point (B) were used (Figure 1A). Maxillomandibular

relationship (ANB), Upper Face Height (N-ANS), Posterior Face Height (S-Go), SN/GoGn and Mandibular Length (Co-Gn) measurements were made using these points (Figure 1B).

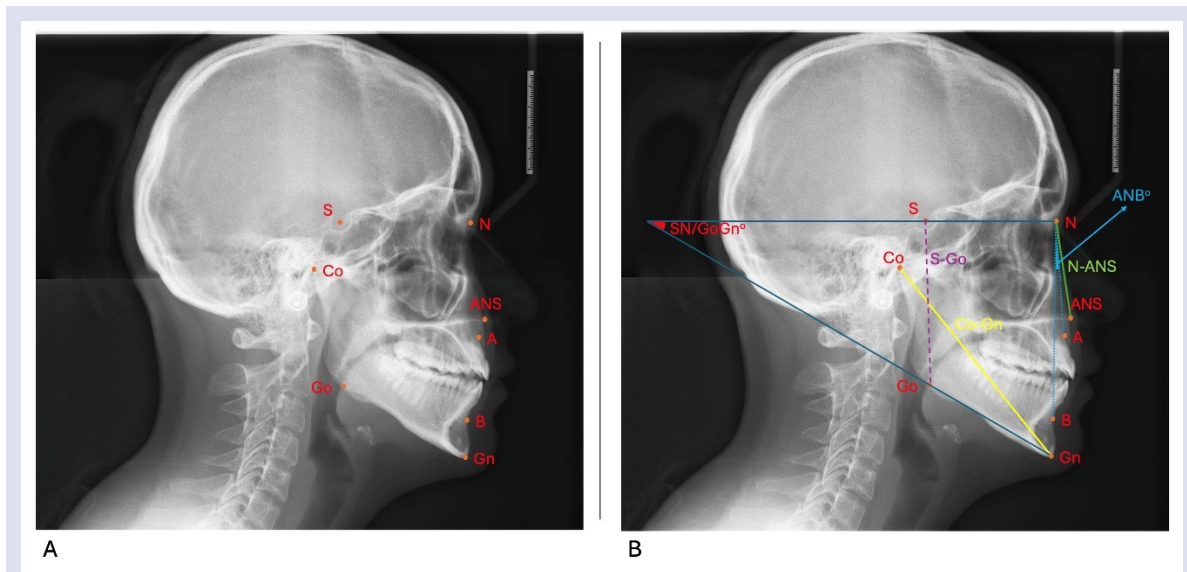


Figure 1: A) Cephalometric points used for analyses. B) Angular and linear measurements used in analysis.

Cone Beam Computed Tomography Parameters

All CBCT images to be scanned were obtained with the New-Tom 5G device (QR, Verona, Italy), at 110 kV and 3–5 mA, with a voxel size of 0.16 mm, a size of 18 × 16 cm, and a typical time of 5.4 s. Examinations and measurements of axial and coronal sections were made with the built-in NNT (New-Tom Image Viewer, QR, Verona, Italy) software.

Crista Galli Measurements

Linear Measurements: By examining the coronal and axial sections of the CBCT images, the height of the CG (linear distance between the cribriform plate in the supero-inferior direction and the top point of the CG) was measured on the coronal sections (Figure 2a). The width in the mediolateral direction (linear distance between the CG cortical outer borders) was measured (Figure 2b). The length (between the frontal bone inner cortex tip and the most posterior point of the CG) was measured by examining the axial section measurements (Figure 2c).⁸

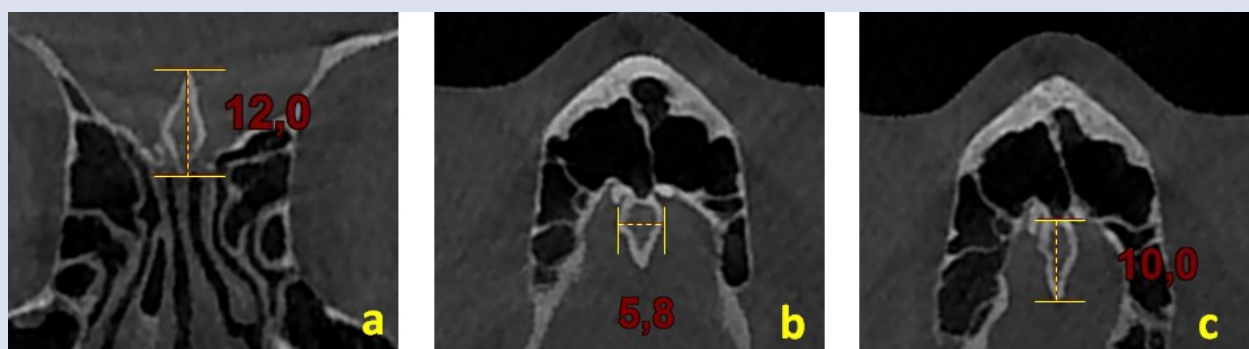


Figure 2: CG measurements. a) Measurement of the height of the CG on coronal CBCT slice. b) Measurement of the width of the CG on axial CBCT slice. c) Measurement of the length of the CG on axial CBCT slice.

Morphology of the Crista Galli: This assessment utilized the Crista Galli (CG) measurements outlined by Komut et al. in 2022, alongside the classification system based on the presence of the cavitory component (see Figure 3).⁷ This analysis was conducted utilizing axial and coronal

sections from Cone Beam Computed Tomography (CBCT) scans. According to this classification system: Type 1 (teardrop type) denotes a CG width exceeding one-third of its height, characterized by a prominent cavitory component (refer to Figure 3a). Type 2 (tubular type)

indicates a width less than one-third of the height, with a cavitory component extending from the base to the top (see Figure 2b). Type 3 (ossified type) features a width less than one-third of its height, lacking a discernible cavitory component (depicted in Figure 3c).^{7,8} Additionally, the Keros classification, which assesses the depth of the olfactory fossa relative to the height of the lateral lamella

of the cribriform plate (CP), delineates: 1-3 mm for type 1 (where CP and ethmoid roof (ER) are aligned at the same level, as illustrated in Figure 4a), 4-7 mm for type 2 (as depicted in Figure 4b), and 8-12 mm for type 3 (with CP notably situated downstream of ER, as shown in Figure 4c). Furthermore, the presence of pneumatization within the CG was also scrutinized (refer to Figure 5).⁷

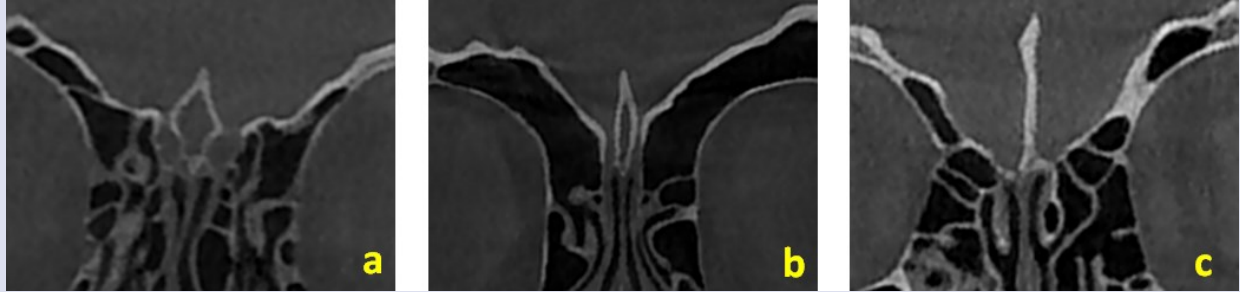


Figure 3: Morphological classification of CG on coronal CBCT slices. a) Teardrop type. b) Tubular type. c) Ossified type.

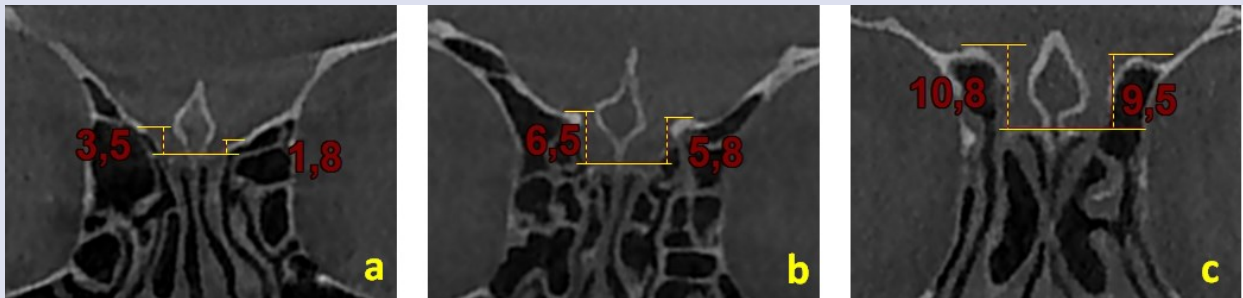


Figure 4: Keros classification types of the CG on coronal CBCT slices. a) Keros type 1. b) Keros type 2. c) Keros type 3.

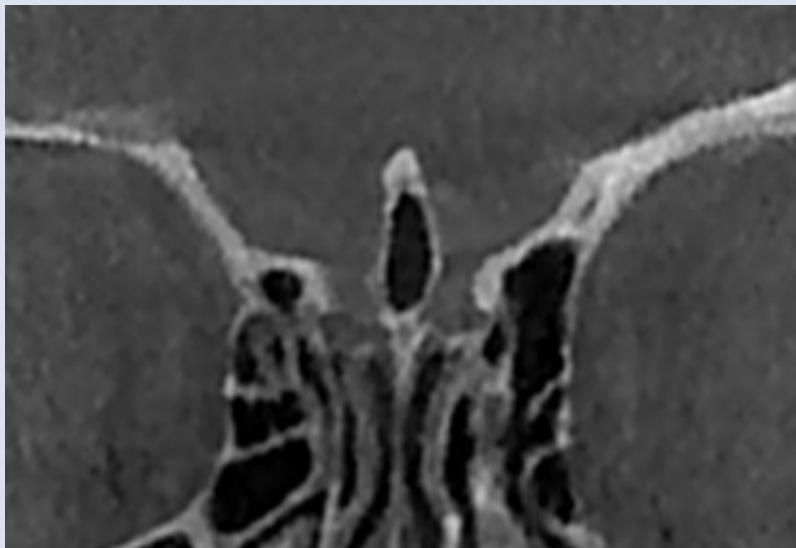


Figure 5: Pneumatized crista galli on coronal CBCT slice.

Statistical Analysis

The Jamovi (version 2.4.8.0, Sydney, Australia) statistical analysis software was used for statistical evaluation of the data.¹⁸ The Pearson chi-square was used

to evaluate categorical data. The Shapiro–Wilk test was used in the normality analysis of the numerical data. The Kruskal–Wallis test (Mann–Whitney U test for post hoc pairwise comparisons) was used in the comparison

between groups of non-parametric variables. One-way ANOVA was used for parametric variables. Spearman correlation coefficients were used to examine the correlations between variables. Linear regression analysis was used to determine the factors affecting CG morphometry. Ordinal logistic regression analysis was used to describe the relationships between skeletal malocclusion classes and CG morphometry and morphology. The statistical significance value was taken as $p < 0.05$.

Results

The comparisons of CG morphometry and morphology of the skeletal malocclusion classes are given in Table 1. When the linear measurements of the CG were evaluated, no difference was found between skeletal malocclusion classes in terms of width ($p=0.782$) or height ($p=0.595$).

In contrast, the CG length was significantly ($p=0.048$) greater in Class I individuals. On the other hand, the CG length of Class I and Class II individuals (11.67 ± 2.28 mm) is similar. No significant relationships existed of CG morphology ($p=0.160$), Keros classification ($p=0.730$), and CG pneumatization ($p=0.594$) with skeletal malocclusion groups.

The significant relationships between CG linear measurements and cephalometric parameters, controlling for skeletal class, are given in Table 2. Weakly positive significant correlations existed between CG length and Co-Gn ($Rho=0.475$, $p < 0.01$) and S-Go ($Rho=$

0.233 , $p < 0.05$) lengths. Weakly positive significant correlations were found between CG width and S-Go length ($Rho=0.301$, $p < 0.05$). A weakly positive significant correlation existed between CG height and N-ANS ($Rho=0.314$, $p < 0.05$). Although significant positive correlations were found between CG width and height ($Rho=0.359$, $p < 0.05$), no significant correlation existed between these measurements and CG length.

The linear regression analysis results of the CG linear measurements are given in Table 3. When the CG morphology type was ossified, the CG length decreased by 3.32 times ($p=0.016$). When the CG length increased by 1 unit, the SN/GoGn angle decreased by 0.20 times ($p=0.046$), and the CG height increased by 0.37 times ($p=0.015$). When the CG width was examined according to CG morphology, it decreased 1.82 times ($p=0.003$) when it was tubular type and 3.27 times ($p=0.002$) when it was ossified type. When the CG width increased by 1 unit, the CG height increased by 0.32 units ($p=0.006$). When the CG height is examined according to CG morphology, it increased by 2.95 times ($p=0.009$) when it was tubular type and 4.86 times ($p=0.013$) when it was ossified type.

The results of the ordinal logistic regression analysis examining the relationships between skeletal malocclusion category and CG morphometry and morphology measurements are presented in Table 4 (overall model test, $p=0.023$). When examined by skeletal class, CG length ($p=0.008$) and gender ($p=0.009$) were important risk factors for malocclusion.

Table 2. Correlation matrix for crista galli linear measurements.

		CG Length	CG Width	CG Height
CG Width	Pearson's r	0.201	—	
	Spearman's rho	0.252	—	
CG Height	Pearson's r	0.272	0.332*	—
	Spearman's rho	0.171	0.359*	—
Co-Gn	Pearson's r	0.403**	0.187	-0.01
	Spearman's rho	0.475**	0.18	-0.053
S-Go	Pearson's r	0.310*	0.251	-0.007
	Spearman's rho	0.233*	0.301*	-0.051
N-ANS	Pearson's r	0.042	0.175	0.293
	Spearman's rho	0.107	0.175	0.314*

Note: Checked for skeletal class. * $p < 0.05$. ** $p < 0.01$.

Table 3. Linear regression model results for crista galli linear measurements.

	Variables		Estimate	%95 CI		P values	R ²	Adjusted R ²	Overall Model Test	
				Lower	Upper				F	p
CG Length	CG	2-1	-0.67	-2.43	1.08	0.432	0.792	0.518	2.89	0.010*
	Morphology	3-1	-3.32	-5.95	-0.70	0.016				
	SN/GoGn		-0.20	-0.39	-0.01	0.046				
CG Width	CG Height		0.37	0.08	0.65	0.015	0.769	0.466	2.53	0.021*
	CG	2-1	-1.82	-2.95	-0.70	0.003				
	Morphology	3-1	-3.27	-5.15	-1.38	0.002				
CG Height	CG Height		0.32	0.10	0.54	0.006	0.751	0.422	2.29	0.034*
	CG	2-1	2.95	0.83	5.07	0.009				
	Morphology	3-1	4.86	1.15	8.57	0.013				
	CG Length		0.75	0.16	1.33	0.015				
	CG Width		1.03	0.33	1.73	0.006				

CI: Confidence Interval. Type 1 was the reference category for CG morphology. * $P < 0.05$; ** $P < 0.01$; *** $P < 0.001$.

Table 4. Table for ordinal logistic regression analysis between skeletal class and crista galli morphometry and morphology measurements.

Predictor	Estimate	SE	Z	OR	%95 CI		p
					Lower	Upper	
CG length	-0.57	0.21	-2.66	0.57	0.36	0.84	0.008**
CG width	-0.47	0.38	-1.24	0.62	0.28	1.31	0.214
CG height	0.21	0.20	1.04	1.23	0.86	1.91	0.298
Age	0.07	0.05	1.53	1.07	0.98	1.18	0.126
Gender (Male - Female)	2.81	0.82	2.62	8.54	1.096	51.02	0.009**
CG Morphology (Type 2-1)	-1.76	0.95	-1.84	0.17	0.02	1.07	0.066
CG Morphology (Type 3-1)	-4.46	2.38	-1.87	0.01	0.00	0.69	0.061
Keros Classification (Type 2-1)	-0.13	1.06	-0.12	0.88	0.11	7.11	0.904
Keros Classification (Type 3-1)	-0.16	1.36	-0.12	0.85	0.05	11.91	0.905
Pneumatization (Present-Absent)	1.70	1.63	1.04	5.47	0.23	197.55	0.297

Deviance: 78.11. **AIC:** 102.11, $R^2_{McFadden's}$: 0.21, $R^2_{Cox\&Snell's}$: 0.14, $R^2_{Nagelkerke's}$: 0.27. **Overall Model Test:** χ^2 , 20.77, $p=0.023$. **CI:** Confidence Interval. **CG:** Crista Galli. **OR:** Odds Ratio. **Reference category:** Skeletal Class I. * $P < 0.05$; ** $P < 0.01$; *** $P < 0.001$.

Discussion

The ossification of the CG, which is seen as a rooster-comb-like structure on the midline of the cribriform plate of the ethmoid bone in the second month of fetal development, generally begins in the second month after birth and increases until the 14th month, and then gradually progresses until completion in the 24th month.^{1,8,19} This structure, which is closely related to the central structures in the frontal skull base, especially the falx cerebri that separates the right and left cerebral hemispheres, has an extremely important place in endoscopic sinus and skull base surgeries due to its location, shape, and dimensions.^{2,20} The skull base has an important place in the classification and definition of skeletal malocclusions.²¹ Therefore, a relationship may exist between structures involving the skull base and skeletal malocclusions.^{21,22} This study thus aimed to examine the relationship between the CG, located in the anterior part of the skull base, and skeletal malocclusions.

The review study of Gong et al. examined cranial base characteristics in various anteroposterior skeletal malocclusions and reported that cranial base length differed morphologically.²¹ Cranial base lengths were smaller in skeletal class III malocclusion. However, in that study, an examination was provided only from lateral cephalometric radiographs, which provide a two-dimensional view. In our current study, the fact that the anterior-posterior length of the CG of Class I individuals is larger than that of Class III individuals, but has a similar length to Class II individuals, adds another dimension to this information. This adds new information to the literature. Again, in the study of Gong et al.²¹, the cranial base length and angle were smaller in class III individuals than in class I individuals, which somewhat supports our findings.

Amano et al. examined the activity of the neural crest cells that form the anterior craniofacial skeleton and facial structure. They reported that the developmental effect between the nasomaxillary complex and skeletal malocclusions was significant.²³ They revealed that the genes causing hypoplastic nasomaxillary complex are

related to skeletal malocclusion. This may lead us to think that variations in the nasomaxillary complex, which includes the CG and is in proximity, may vary according to skeletal malocclusions. In this context, although a relationship between CG and skeletal malocclusions may be predicted, an exact relationship could not be revealed in our study. Only a difference between skeletal malocclusions in the linear anteroposterior length of the CG was demonstrated. Additionally, the regression analysis determined that the CG length could be seen as a low risk factor in the development of skeletal malocclusion. The main factor affecting the linear measurements of the CG was CG morphology. Among the cephalometric values, only the SN/GoGn angle had a low impact on CG length. Moreover, the presence of a positive correlation between CG width and height in skeletal malocclusion control supports these findings and strengthens the definition of the relationship between them. However, further studies are needed.

A recent study by Chou et al. examined the relationship between cranial base measurements and sagittal skeletal malocclusions.²⁴ In that study, the CG length was examined, and it was like the findings of our study. Consistent with our work, the width of the cribriform plate of the ethmoid bone did not differ between skeletal malocclusions. In the study of Rai et al., referring to the vertical length of the face, they reported that cranial base lengths were longer in individuals with long faces.²⁵ This literature information may provide the idea that there may be a relationship between cranial base lengths and facial length, and that the crista galli located in the anterior cranial base may also be indirectly affected by this. In this study, various relationships were found between CG dimensions and vertical measurement parameters of the face. Additionally, although no correlation existed between the CG and cribriform plate measurements in that study, a significant correlation was found between CG height and width in our study. Our study found a positive correlation between CG length and Co-Gn and S-Go cephalometric measurements and between N-ANS and CG height. These findings suggest a possible weak relationship between skeletal facial length

and height and CG dimensions. Furthermore, there is insufficient information in the literature about the relationship between crista galli and maxillomandibular dimensions. This study constitutes one of the first examples of attribution.

Many studies have examined the relationships between CG morphology and morphometry and gender and the role of this structure in gender determination.⁶⁻⁸ Different from those studies, our study found no difference in CG morphology and morphometry between genders. Therefore, comparisons were made between skeletal malocclusion groups. Additionally, some studies examining gender determination have involved CT examinations, with no examination of skeletal malocclusions.^{6,7} The reason for the lack of gender differences in our study can be considered the number of samples. This provides a limitation, but the fact that our research question was not about gender and that the study represents a guide for further research supports its contribution to the literature. Our study used CBCT, which causes lower radiation exposure than conventional CT devices.^{8,26} The protection of individuals from radiation in line with the ALARA principle was considered²⁷, and the study also aimed to raise awareness for clinicians providing CBCT examinations. In our study, unlike the literature, CG pneumatization was examined but not encountered. The reason for this may be the very low frequency of pneumatization, as stated in the literature, and the sample size of our study. Future studies should focus more on this.

Limitations

One of the main limitations of our study is its low sample size. As a precaution, a power analysis was performed before the study. Additionally, image acquisition in a wide FOV range to enable the CG to be visible is limited, especially in individuals with skeletal class I malocclusion and who have received CBCT for various diagnostic reasons. Our knowledge of health care services, which primarily aims to protect individuals, foresees minimal radiation exposure in line with the ALARA principle.²⁷

Conclusions

- The CG length of skeletal class I individuals is greater than that of class III individuals. The CG length of skeletal Class II individuals is like both Class I and Class III individuals.
- The CG width and height do not differ according to skeletal malocclusion classes.
- CG morphology did not differ according to sagittal skeletal malocclusions.
- A positive correlation existed between the effective mandibular length (Co-Gn) and the anteroposterior length of the CG.
- A weak relationship may exist between certain cephalometric parameters and CG dimensions.

Acknowledgments

Author Contributions Conception or design of the work: Taner Ozturk; Data collection: Yunus Emre Ucaker, Aykagan Cukurluoglu; Data Analysis: Taner Ozturk, Aykagan Cukurluoglu; Drafting the article: Taner Ozturk, Yunus Emre Ucaker; Critical revision of the article: Taner Ozturk; Final approval of the version to be published: Taner Ozturk, Yunus Emre Ucaker, Aykagan Cukurluoglu.

Ethical Approval

The ethical approval required for this retrospective study was obtained from the Erciyes University Clinical Research Ethics Committee (Approval no: 2023/338; Approval date: May 10th, 2023). The study was carried out in accordance with the Declaration of Helsinki, and informed consent forms were obtained from all individuals at the beginning of the study.

Consent to participate

Informed consent was obtained from all individual participants included in the study

Conflict of Interest

The author(s) declared no potential conflicts of interest with respect to the research, authorship, and/or publication of this article.

Funding

None.

References

1. Vuralli D, Polat S, Isik EI, Öksüzler M, Özel AS, Göker P. Crista Galli Morphometry and Morphology: An Anatomical, Radiological, and Machine Learning Application Study. *Int J Morphol.* 2023;41:749-57.
2. Özeren Keşkek C, Aytuğar E. Clinical significance and radiological evaluation of Crista Galli: a CBCT study. *Eur J Anat.* 2021;25:705-11.
3. Danielsen A, Reitan E, Olofsson J. The role of computed tomography in endoscopic sinus surgery: a review of 10 years' practice. *Eur Arch Otorhinolaryngol.* 2006;263:381-9. doi:10.1007/s00405-005-1032-0
4. Tetiker H, Kosar MI, Çullu N, Sahan M, Gençer CU, Derin S. Pneumatization of crista galli in Pre-adult and Adult Stages. *Int J Morphol.* 2016;34:541-4.
5. Akiyama O, Kondo A. Classification of crista galli pneumatization and clinical considerations for anterior skull base surgery. *J Clin Neurosci.* 2020;82:225-30. doi:10.1016/j.jocn.2020.11.005
6. Golpinar M, Salim H, Ozturk S, Komut E, Sindel M. Sex estimation with morphometric and morphological characteristics of the crista galli. *Surg Radiol Anat.* 2022;44:1007-15. doi:10.1007/s00276-022-02971-2
7. Komut E, Golpinar M. A comprehensive morphometric analysis of crista galli for sex determination with a novel morphological classification on computed tomography images. *Surg Radiol Anat.* 2021;43:1989-98. doi:10.1007/s00276-021-02799-2

8. Okumus O. The use of crista galli morphology and morphometry in sex determination: a cone-beam computed tomography study. *Folia Morphol (Warsz)*. 2022;81:1005-13. doi:10.5603/FM.a2022.0077
9. Baydas B, Yavuz I, Durna N, Ceylan I. An investigation of cervicovertebral morphology in different sagittal skeletal growth patterns. *Eur J Orthod*. 2004;26:43-9. doi:10.1093/ejo/26.1.43
10. Leonardi R, Barbato E, Vichi M, Caltabiano M. A sella turcica bridge in subjects with dental anomalies. *Eur J Orthod*. 2006;28:580-5. doi:10.1093/ejo/cjl032
11. Newaz ZA, Barghan S, Katkar RA, Bennett JA, Nair MK. Incidental findings of skull-base abnormalities in cone-beam computed tomography scans with consultation by maxillofacial radiologists. *Am J Orthod Dentofacial Orthop*. 2015;147:127-31. doi: 10.1016/j.ajodo.2014.09.019.
12. Kose SK, Aksoy S, Onder M, Oz U, Orhan K. Association among Orthodontic Malocclusions, Paranasal Sinuses Anatomic Variations and Adenoid Vegetation in Children Using CBCT. *Children*. 2023;10:1549. doi: 10.3390/children10091549
13. Tindlund RS, Holmefjord A, Eriksson J-CH, Johnson GE, Vindenes H. Interdisciplinary Evaluation of Consecutive Patients With Unilateral Cleft Lip and Palate at Age 6, 15, and 25 Years: A Concurrent Standardized Procedure and Documentation by Plastic Surgeon; Speech and Language Pathologist; Ear, Nose, and Throat Specialist; and Orthodontist. *J Craniofac Surg*. 2009;20:1687-98. doi:10.1097/SCS.0b013e3181b3edb5
14. Gruszka K, Aksoy S, Różyło-Kalinowska I, Gülbeş MM, Kalinowski P, Orhan K. A comparative study of paranasal sinus and nasal cavity anatomic variations between the Polish and Turkish Cypriot Population with CBCT. *Head Face Med*. 2022;18:37. doi: 10.1186/s13005-022-00340-3.
15. Aranitasi L, Tarazona B, Zamora N, Gandía JL, Paredes V. Influence of skeletal class in the morphology of cervical vertebrae: A study using cone beam computed tomography. *Angle Orthod*. 2016;87:131-7. doi:10.2319/041416-307.1
16. Algahefi AI, Alhammadi MS, Zheng B, Almashraqi AA, Zhao Y, Liu Y. Morphological and dimensional variations of the frontal air sinuses in a group of adolescent Caucasians and Chinese in different skeletal malocclusions: a cross-sectional cephalometric study. *Clin Oral Invest*. 2022;26:5711-9. doi:10.1007/s00784-022-04527-5
17. Turker G, Ozturk T, Coban G, Isgandarov E. Evaluation of Various Sagittal Cephalometric Measurements in Skeletal Class I Individuals with Different Vertical Facial Growth Types. *Forum Ortod*. 2021;106-13. doi: 10.5114/for.2021.107530
18. The jamovi project. jamovi (Version 2.3) [Computer Software]. 2023. <https://www.jamovi.org>
19. Hajiioannou J, Owens D, Whittet HB. Evaluation of anatomical variation of the crista galli using computed tomography. *Clin Anat*. 2010;23:370-3. doi:10.1002/ca.20957
20. Lee JM, Ransom E, Lee JY, Palmer JN, Chiu AG. Endoscopic anterior skull base surgery: intraoperative considerations of the crista galli. *Skull Base*. 2011;21:83-6. doi:10.1055/s-0030-1263283
21. Gong A, Li J, Wang Z, et al. Cranial base characteristics in anteroposterior malocclusions: A meta-analysis. *Angle Orthod*. 2016;86:668-80. doi:10.2319/032315-186.1
22. Dhopatkar A, Bhatia S, Rock P. An Investigation Into the Relationship Between theCranial Base Angle and Malocclusion. *Angle Orthod*. 2002;72:456-63. doi: 10.1043/0003-3219(2002)072<0456:AIITRB>2.0.CO;2.
23. Amano K, Okuzaki D, Aikawa T, Kogo M. Indian hedgehog in craniofacial neural crest cells links to skeletal malocclusion by regulating associated cartilage formation and gene expression. *FASEB J*. 2020;34:6791-6807. doi: doi: 10.1096/fj.201903269R
24. Chou S-T, Lin S-H, Chen S-C, Chen C-M, Tseng Y-C. Comparison of the transverse cranial base dimension in different craniofacial skeletal relationships: A cone-beam computed tomography study. *J Dent Sci*. 2024;19:364-76. doi: 10.1016/j.jds.2023.07.018
25. Rai S, Saidath K, Mathew KA, Shetty SS. Assessment and comparison of cranial base morphology in individuals with long face and short face. *J Orthod Sci*. 2023;12(1):30. doi: 10.4103/jos.jos_187_21.
26. Costa ALF, Paixao AK, Goncalves BC, et al. Cone Beam Computed Tomography-Based Anatomical Assessment of the Olfactory Fossa. *Int J Dent*. 2019;2019:4134260. doi:10.1155/2019/4134260
27. Lurie AG. Doses, Benefits, Safety, and Risks in Oral and Maxillofacial Diagnostic Imaging. *Health Phys*. 2019;116:163-169. doi:10.1097/hp.0000000000001030